Current-induced one-dimensional diffusion of Co adatoms on graphene nanoribbons

Preis, T.; Vrbica, S.; Eroms, J.; Repp, J.; Ruitenbeek J.M. van

NANO LETTERS

pubs.acs.org/NanoLett

Letter

Current-Induced One-Dimensional Diffusion of Co Adatoms on Graphene Nanoribbons

Tobias Preis, Sasha Vrbica, Jonathan Eroms, Jascha Repp, and Jan M. van Ruitenbeek*

Cite This: *Nano Lett.* 2021, 21, 8794–8799

Read Online

ACCESS | Metrics & More | Article Recommendations

ABSTRACT: One-dimensional diffusion of Co adatoms on graphene nanoribbons has been induced and investigated by means of scanning tunnelling microscopy (STM). To this end, the nanoribbons and the Co adatoms have been imaged before and after injecting current pulses into the nanoribbons, with the STM tip in direct contact with the ribbon. We observe current-induced motion of the Co atoms along the nanoribbons, which is approximately described by a distribution expected for a thermally activated one-dimensional random walk. This indicates that the nanoribbons reach temperatures far beyond 100 K, which is well above the temperature of the underlying Au substrate. This model system can be developed further for the study of electromigration at the single-atom level.

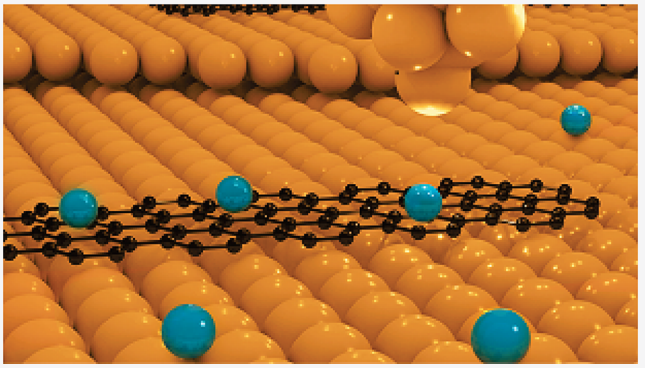

KEYWORDS: *adatom diffusion, graphene nanoribbons, scanning tunneling microscopy, electromigration*

Graphene nanoribbons (GNR) can be engineered with atomic perfection by on-surface synthesis from molecular precursors,[1] offering a rich variety of fascinating electronic properties.[2−6] Their band gap can be tuned by the physical width of the ribbon, such that they represent nearly ideal model systems for investigating one-dimensional (1D) electron transport.[7,8] GNR can be intrinsically doped by adsorption onto a surface with a different work function[9−12] or by substituting carbon atoms in the lattice.[13,14] Alternatively, dopants can be deposited onto the GNR,[15,16] but little is known of how a current flow through GNR may affect adsorbed dopants.[17] Here, we demonstrate that high current densities will drive dopant atoms to diffuse, at bath temperatures for which thermal diffusion is inhibited. Interestingly, the diffusion is confined to the GNR, rendering GNR unique for studies of atomic diffusion in one dimension. We anticipate that the system can be further developed as a model system for studying electromigration at the atomic scale and testing fascinating predictions.[18,19] STM experiments were carried out under ultrahigh vacuum at low temperatures T of 7−10 K, unless specified otherwise. Images were acquired at constant current of I = 2 pA at a bias voltage V = ± 100 mV, referring to the sample voltage with respect to the tip. The tip was made from a 20 μm thick PtIr wire, conditioned by controlled indentations into the clean gold surface, producing atomically sharp gold-coated tips. A Au(111) single-crystal surface was cleaned by Ne^+ ion sputtering, followed by thermal annealing at 550 °C. GNR on Au(111) were synthesized following ref 1, resulting in 7-carbon-dimers-wide ribbons with armchair edges (7-aGNR). Subsequently, Co atoms were coadsorbed onto the cold (≃ 15 K) surface. A significant fraction of them is adsorbed on top of the GNR, see Figure 1a.

GNR fabricated by this method[1,20] have a uniform width but vary in length. Whereas Co on Au(111) has an apparent height of 0.1 nm in the STM images, Co adatoms on a GNR show an apparent height of 0.23 nm. A similar increase in apparent height is also observed on ultrathin insulating layers.[21] Occasionally, some Co-atom-related protrusions on GNR appear even larger—about 0.35 nm high (Figure 1b,c). They may be due to dimers, hydrogen attachment, or different adsorption,[22] and are disregarded here.

At T ∼ 7 K, the Co atoms and the GNR remain stationary. To determine the preferred adsorption site, the center position of Co adatoms as well as the central axis of a GNR were extracted from suitable fitting procedures of the images. From this analysis, we find only adsorption at positions A, B, D, and E (see inset in Figure 1a), consistent with Co preferentially adsorbing at the centers of the outer carbon rings of the GNR, in agreement with ref 23.

Received: August 16, 2021
Revised: September 24, 2021
Published: October 15, 2021

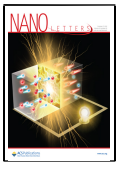

https://doi.org/10.1021/acs.nanolett.1c03073
Nano Lett. 2021, 21, 8794–8799

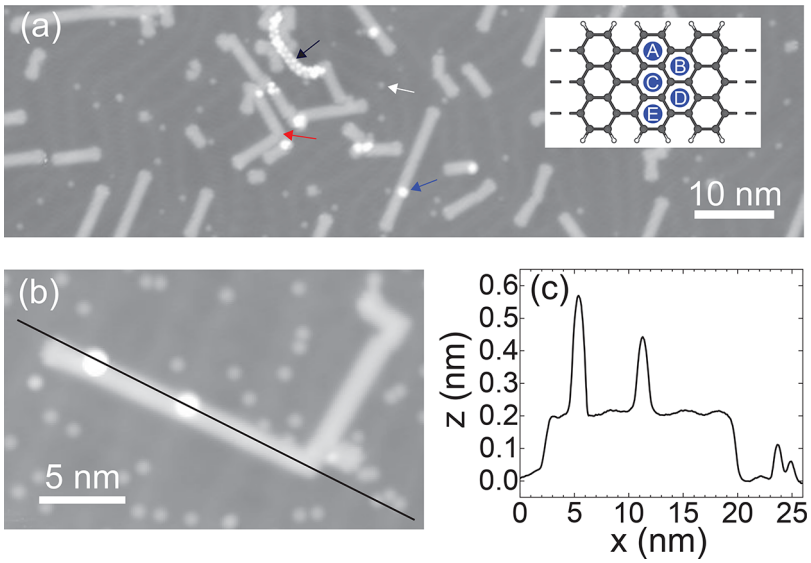

Figure 1. Overview of GNR and coadsorbed Co adatoms on Au(111). (a) Large-area STM image of the sample after cobalt adatom deposition. Some GNR are not fully flattened out from dehydrogenation (black arrow), and a few GNR are kinked (red arrow) or deviate otherwise from their ideal 1D structure. Most Co adatoms are located on clean areas of Au (white arrow), while a few are located on top of GNR (blue arrow). The inset shows the geometric structure of the GNR along with the five possible ring-centered adsorption sites per unit cell. (b) STM image of a GNR decorated by two Co adatoms. (c) Line profile along one arm of the kinked GNR, indicated by the black line in (b).

The current injection with the STM tip into GNRs to induce motion of the adatoms is performed as follows. The STM tip is positioned above a suitable GNR at a lateral distance s from a Co atom, indicated by the green dot in Figure 2c.

Next, the feedback is switched off and the tip is lowered (z decreases; blue curve in Figure 2a). The tunneling current, Figure 2b, rises exponentially with decreasing tip−sample distance until a kink (observed in most traces) indicates a jump to contact.[24,25] The tip approach is continued for another 0.02−0.03 nm to ensure stable contact. In contact, the sample voltage is ramped up, briefly maintained at V_{max} and then ramped down to its initial value, over a total duration of 1 s (see Figure 2a). Afterward, the tip is retracted and another STM image is taken; an example is shown in Figure 2c. By comparing the images before and after the pulse the displacement d of the Co atom is determined. $d > 0$ indicates a displacement away from the tip. The high-bias resistance of the junction in contact does not depend systematically on voltage polarity, nor on the distance to a Co adatom.

We applied over 900 pulses on GNRs and recorded a total of 1430 events (a single pulse may affect multiple Co adatoms). Remarkably, after application of a pulse, roughly half of the Co atoms investigated are displaced to a new position on the same GNR (see Table 1). Atoms can be displaced toward or away from the tip, for either voltage polarity, and the average displacement is quite significant, averaging at 3−4 graphene hollow sites. Only in very few cases were Co atoms found to be moved from the GNR to the bare Au surface. Finally, roughly 7% of the atoms disappeared from the image after the pulse. We assume that they must have been picked up by the tip. We restrict the analysis to experiments for voltage pulses $|V| \geq 600$ mV. We also exclude data for which the tip−sample resistance remained larger than 330 kΩ upon contact. Atoms located at the end points of the GNR or at kink sites are disregarded.

Figure 3a shows the escape probability of Co adatoms on GNRs after a voltage pulse, as a function of the initial tip−adatom distance s. We define the escape probability as the ratio of the atoms that are displaced (excluding those that have presumably been picked up by the tip), to the total number of Co atoms traced. The data are grouped in intervals of s, and a data point at s combines data for the interval from $s - 1$ nm to $s + 1$ nm. Clearly, atoms closer to the tip are more likely to be displaced.

Figure 3b shows the escape probability as a function of V_{max}, extracted from all data for $s < 10$ nm, since the dependence on s in this range is small. Each data point represents an interval of 0.1 V. Despite some scatter, we can recognize a trend of increasing escape probability for increasing bias voltage.

Figure 4 shows a histogram of the distance d by which adatoms are displaced as a result of a pulse, extracted from all data with $|V| \geq 0.6$ V. The red curve is a fit of the histogram, excluding the anomalous bin at $d = 0$, to $P(d) = Ae^{-(d-d_0)^2/w^2}$. The center of the distribution lies at zero, to within the statistical accuracy, $d_0 = 0.1 \pm 0.8$ nm, as expected for a random-walk probability distribution. The width $w^2 = 1.0$ nm^2 suggests an average number of hopping events per pulse of 13. Although the fit appears to match the data reasonably well on a linear scale, a semilog plot (see inset) reveals deviations at larger distances. The events with $d > 3$ nm appear orders of magnitude more frequently than expected from the simple 1D random walk. We return to these long tails and the anomalously large peak at $d = 0$ below.

The Co atoms on the Au substrate in the vicinity of the GNR occasionally are also displaced after a voltage pulse. We performed additional experiments for Co atom migration resulting from voltage pulses applied on the bare Au surface,[26,27] which turned out to be useful for better understanding the origin of atom migration on the GNR, by comparison. By using the same pulsing scheme as for GNR and restricting this comparison to $s \leq 7$ nm, we observe that adatoms are much less frequently displaced for pulses directly on gold, namely only 3% (16 of 519 atoms).

To compare the effect of voltage-pulse-induced atom migration to thermal activation, we performed a series of

https://doi.org/10.1021/acs.nanolett.1c03073
Nano Lett. 2021, 21, 8794−8799

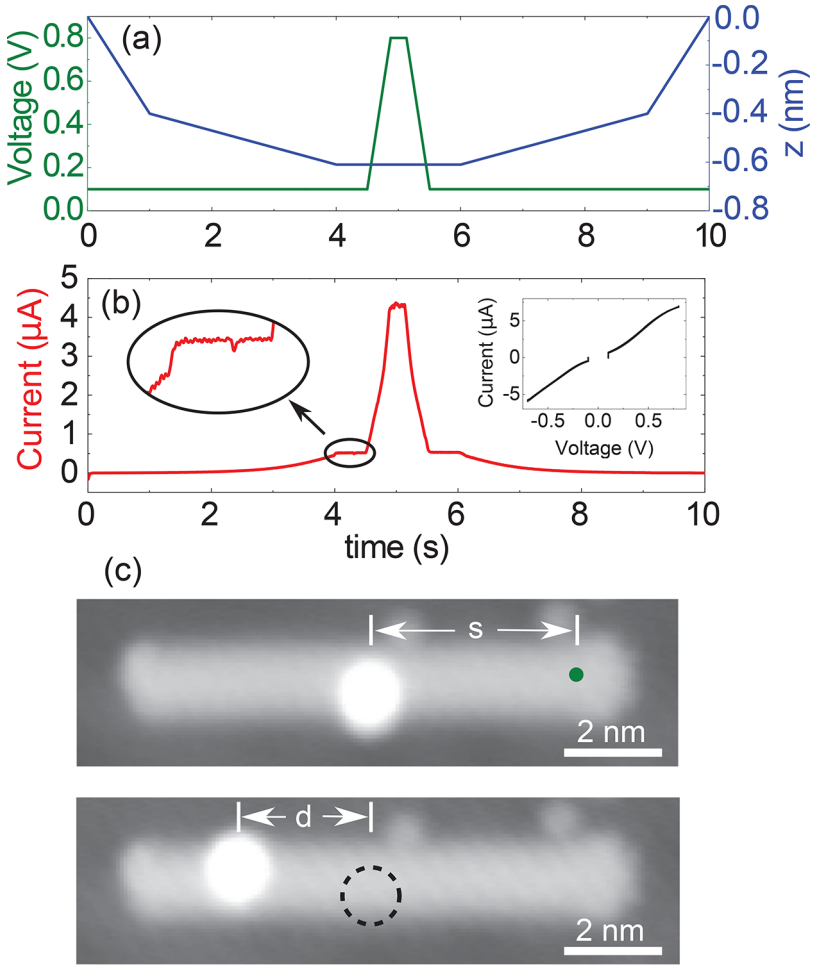

Figure 2. Procedure of current-pulse injection. (a) The blue curve indicates the tip approach toward the GNR. A voltage pulse is applied in contact, here 0.8 V for a duration of 0.5 s (green curve). (b) Tunneling current recorded during the pulse. An abrupt increase indicates the jump to contact, as shown on a 3.7× magnified scale in the inset. The current is seen to rise nearly linearly with the voltage (right inset). The curves shown here are representative for all the data, at both voltage polarities. (c) STM images of a GNR before (top) and after (bottom) the voltage pulse for V_{max} = 0.8 V. The green dot on the GNR marks the tip position for the applied voltage pulse, at a distance *s* from the adatom's initial position. After the pulse, the Co adatom has moved away from the tip over a distance *d*, as observed in the lower image.

Table 1. Statistics for Co Motion after a Voltage Pulse

response to voltage pulses of Co adatoms on GNRs	number	% of total
total number of Co atoms traced	1430	100%
number of Co atoms that did not move	736	51.5%
number of displaced Co atoms (including events below)	694	48.5%
Co moved along GNR	536	37.5%
Co dropped to Au surface	6	0.4%
Co moved to other edge (between sites A and E)	54	3.8%
Co atom disappeared (pick up by STM tip)	98	6.8%

experiments at elevated temperatures T (raised in steps of ∼15 K) by heating the STM head. At each temperature, from drift-corrected sequences of STM images of the same surface area, we analyzed the diffusion of the adatoms.[28]

Thermally activated displacement of Co atoms on the bare gold surface was first detected at $T \sim 34$ K. At even higher temperatures, the high mobility complicates quantitative analysis of the images. However, up to $T = 79$ K, motion of Co on GNRs was not observed. Hence, the diffusion barrier for Co adatoms on GNRs is much higher than that for Co on Au(111). On the basis of the observed diffusion rate of Co/Au(111) at 34 K and assuming a common attempt frequency of $\nu_0 = 10^{13}\,s^{-1}$, we estimate the diffusion barrier of Co on Au(111) to be $E_D^{Au} = 0.10$ eV in agreement with a theoretical study.[29] As mentioned above, for current injection, we observed a rather low escape rate for Co atoms directly adsorbed on Au, indicating that current-induced heating keeps the temperature of the gold surface well below 40 K, in agreement with the large thermal conductivity of bulk Au.

We now turn to a discussion of the observed adatom hopping on GNRs. Remarkably, upon activation by a voltage pulse, the Co atoms diffuse along the GNR and only drop to the Au surface in exceptional cases. This suggests the presence of an Ehrlich−Schwoebel barrier at the GNR edges. The absence of a preferential direction of motion suggests that the motion is activated by current-induced heating of the GNR.[30−35] Adopting a theoretical value of about $E_D^{GNR} \approx 0.5$ eV for the diffusion barrier for Co on single layer graphene from theory (see ref 36 and references therein), we can use the observed hopping rate ν during a pulse, $\nu \sim 25\,s^{-1}$, for estimating the effective temperature on the GNR. Here, we have calculated ν from the average number of hopping events, $N = 13$ (see above), and the typical pulse duration of 0.5 s. Through the Arrhenius law $\nu = \nu_0 \exp(-E_D/(k_B T))$, we obtain

https://doi.org/10.1021/acs.nanolett.1c03073
Nano Lett. 2021, 21, 8794−8799

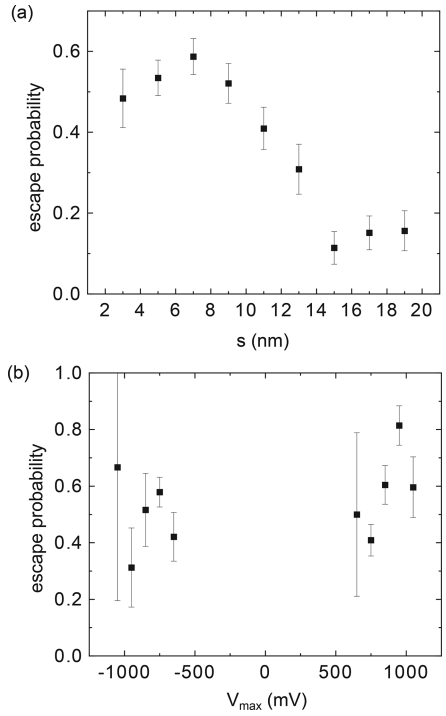

Figure 3. Escape probability (a) as a function of initial tip-adatom separation and (b) as a function of pulsing voltage, for pulses with $s <$ 10 nm. Error bars show the standard deviation.

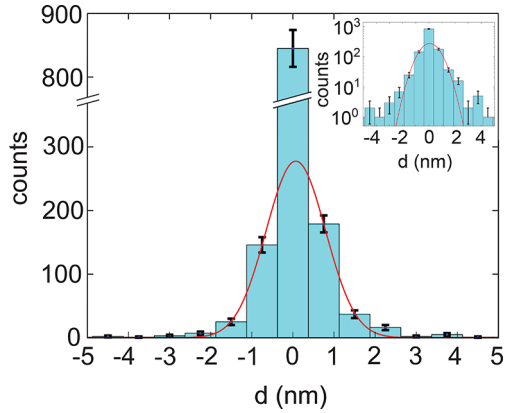

Figure 4. Histogram of the distance d traveled by Co adatoms along the GNR after a voltage pulse, with $t_p \simeq 0.5$ s. Positive (negative) d indicates motion away from (toward) the tip, while $d = 0$ nm indicates Co adatoms that did not move. The red curve shows a fit of the data to a 1D random walk probability distribution, eq 1 with $N \approx 13$, excluding the data points for $d = 0$. The inset shows the data on a semilog scale, emphasizing the deviations to the fit for large displacements d.

a pulse-induced effective temperature $T_{eff} \simeq 200$ K (with an uncertainty ±20 K), which is indeed much higher than the temperatures that we were able to explore by direct heating of the STM.

Provided that the current-induced diffusion can be regarded as analogous to thermally driven diffusion,[37] our observations can be interpreted as follows. The escape probability, Figure 3a, being nearly constant up to ~8 nm, and only dropping by a factor of ~4 at 20 nm, suggests that the effective temperature of the GNR during a pulse is raised above that of the substrate, and is nearly homogeneous over long distances. The exponential dependence of hopping rate with temperature permits a drop of T_{eff} by only about 10 K at the largest distance $s = 20$ nm—small compared to the estimated T_{eff} of 200 K. This picture is consistent with known thermal transport properties: if we simplify and assume that the Au substrate remains uniformly at the base temperature, the balance between thermal transport along the GNR and heat transport into the substrate leads to a decay of temperature with distance s as, $T(s) = T_m \exp(-s/\lambda) + T_0$, for an infinitely long GNR. Here, T_m is the maximum temperature at the tip position, and the decay length is $\lambda = \sqrt{\kappa b/G}$. For the thermal conductivity of graphene we use $\kappa = 200$ W/Km,[38,39] appropriate for 200 K and for the typical length of 10−20 nm of our GNRs. For the thickness $b = 0.144$ nm of graphene, this is equivalent to a two-dimensional thermal conductivity of $\kappa_\square = 30$ nW/K. For the Kapitza interface conductivity we take the value for the interface between graphite and Au,[40] $G = 30 \cdot 10^6$ W/m^{2}K. From these two competing thermal conductivities we find a decay length of $\lambda = 31$ nm for the temperature along the ribbons, supporting the assessment that T_{eff} is nearly constant along the GNR, consistent with experiments for Co metal islands on Cu.[41]

Turning back to the distribution of hopping distances in Figure 4, in case of thermal activation we expect the distribution to be closely approximated by that for a 1D random walk, for which the probability for an atom to move by n lattice sites, $P(n)$, in the limit of large numbers of jumps, N, takes the form,[42]

$$P(n) = \sqrt{\frac{2}{N\pi}}\, e^{-n^2/2N} \tag{1}$$

The histogram in Figure 4 agrees with such a description for short hopping distances, but the large peak at $d = 0$ and the large displacements up to $d = 8$ nm are clearly incompatible. Likely, these deviations result from the variations in effective temperatures between pulses. The currents resulting from a voltage pulse vary because of variations in the contact resistance between tip and GNR. In addition, the total length of the GNR determines the interface area with the Au substrate for thermal relaxation and is expected to influence T_{eff}. The diffusion rate is exponentially sensitive to variations in T_{eff}. For example, a reduction of T_{eff} by only 20 K yields an average number of hops during a pulse below 1, which would explain the large peak at $d = 0$. Similarly, a deviation from $T_{eff} \simeq 200$ K by only 20 K to higher temperatures is compatible with hopping to distances as large as 8 nm. Despite these uncertainties, the global behavior is in agreement with thermally activated 1D diffusion.

We find no polarity dependence in adatom diffusion along the GNR. Directional asymmetry could result from electromigration forces. Electromigration has been widely studied, notably for current-carrying carbon nanotubes.[43] However, it is difficult to obtain access to the effects truely at the atomic scale. Here, we conventionally distinguish a direct force and a wind force.[44] The direct force arises from the effective charge of the Co adatom in the electric field at the surface. The horizontal component of the field should be very small, because of the large effective tip radius, on the order of 50 nm, and the boundary conditions imposed by the Au surface. (Note that the effective tip radius relevant for tunneling is different from the tip radius for electrostatics.) For an adatom sitting 0.3 nm above the image plane, at a distance $s = 10$ nm

https://doi.org/10.1021/acs.nanolett.1c03073
Nano Lett. 2021, 21, 8794−8799

from the point of tunneling, and for a tip−sample potential difference of 1 V, the horizontal component of the electric field can be estimated as 2×10^6 V/m. For a charge of 0.5 e on the adatom,[36] the force would be 0.16 pN. The resulting difference in left and right barrier heights would be $\Delta E = 0.2$ meV, and at $T_{eff} \sim 200$ K, the ratio of left and right jumps would be 0.988. With $N = 13$ this would lead to an expected average displacement of $\bar{d} = 0.16$ nm. Although this shows that we cannot resolve the effect from our data, it suggests that the directional component should be detectable by improving the statistics. The wind force is expected to be very small in our experiment because the 7-aGNR has a band gap of about 2.5 eV.

In summary, we have shown that 7-aGNR on Au(111) serve as nearly perfect 1D channels for Co adatom diffusion. Current pulses injected from an STM tip can be used to heat the GNR, and the statistics of adatom diffusion suggests that this leads to a nearly homogeneous temperature of the GNR. This temperature is remarkably high and far from equilibrium with the underlying Au substrate. The GNR may serve as a model system for single organic molecules connected between metallic leads, for which previous experiments indicated similar high temperatures excited by the transport current,[45] where this temperature cannot be directly measured. Further elaboration of this platform of STM observation of adatom diffusion on GNRs can serve as a nearly ideal model system for the study of electromigration at the atomic scale. Parameters obtained from computational studies for adatoms on graphene suggest that the experiment can be set up to achieve the required current densities.[46] Relevant adjustements would include replacing our 7-aGNR by nanoribbons with a small band gap, such as 5-aGNR[47,48] or 9-aGNR,[49] and arranging the GNR over the edge of thin insulating islands.[8]

AUTHOR INFORMATION

Corresponding Author

Jan M. van Ruitenbeek − *Huygens-Kamerlingh Onnes Laboratory, Leiden University, 2333 CA Leiden, The Netherlands;* orcid.org/0000-0003-0381-0132; Email: ruitenbeek@physics.leidenuniv.nl

Authors

Tobias Preis − *Institute of Experimental and Applied Physics, University of Regensburg, 93040 Regensburg, Germany*

Sasha Vrbica − *Huygens-Kamerlingh Onnes Laboratory, Leiden University, 2333 CA Leiden, The Netherlands*

Jonathan Eroms − *Institute of Experimental and Applied Physics, University of Regensburg, 93040 Regensburg, Germany;* orcid.org/0000-0003-2212-9537

Jascha Repp − *Institute of Experimental and Applied Physics, University of Regensburg, 93040 Regensburg, Germany*

Complete contact information is available at: https://pubs.acs.org/10.1021/acs.nanolett.1c03073

Notes

The authors declare no competing financial interest.

ACKNOWLEDGMENTS

This work is part of the research program of the Netherland's Organization for Scientific Research, NWO. Funding from the Deutsche Forschungsgemeinschaft (DFG, German Research Foundation) through SFB 689, project A07 and 314695032/CRC 1277, projects A09 and B01 is gratefully acknowledged.

REFERENCES

(1) Cai, J.; Ruffieux, P.; Jaafar, R.; Bieri, M.; Braun, T.; Blankenburg, S.; Muoth, M.; Seitsonen, A. P.; Saleh, M.; Feng, X.; Müllen, K.; Fasel, R. Atomically precise bottom-up fabrication of graphene nanoribbons. *Nature* **2010**, *466*, 470−473.

(2) Rizzo, D. J.; Veber, G.; Cao, T.; Bronner, C.; Chen, T.; Zhao, F.; Rodriguez, H.; Louie, S. G.; Crommie, M. F.; Fischer, F. R. Topological band engineering of graphene nanoribbons. *Nature* **2018**, *560*, 204−208.

(3) Gröning, O.; Wang, S.; Yao, X.; Pignedoli, C. A.; Borin Barin, G.; Daniels, C.; Cupo, A.; Meunier, V.; Feng, X.; Narita, A.; Müllen, K.; Ruffieux, P.; Fasel, R. Engineering of robust topological quantum phases in graphene nanoribbons. *Nature* **2018**, *560*, 209−213.

(4) Slota, M.; Keerthi, A.; Myers, W. K.; Tretyakov, E.; Baumgarten, M.; Ardavan, A.; Sadeghi, H.; Lambert, C. J.; Narita, A.; Müllen, K.; Bogani, L. Magnetic edge states and coherent manipulation of graphene nanoribbons. *Nature* **2018**, *557*, 691−695.

(5) Nguyen, G. D.; et al. Atomically precise graphene nanoribbon heterojunctions from a single molecular precursor. *Nat. Nanotechnol.* **2017**, *12*, 1077−1082.

(6) Jacobse, P. H.; Kimouche, A.; Gebraad, T.; Ervasti, M. M.; Thijssen, J. M.; Liljeroth, P.; Swart, I. Electronic components embedded in a single graphene nanoribbon. *Nat. Commun.* **2017**, *8*, 119.

(7) Koch, M.; Ample, F.; Joachim, C.; Grill, L. Voltage-dependent conductance of a single graphene nanoribbon. *Nat. Nanotechnol.* **2012**, *7*, 713−717.

(8) Jacobse, P. H.; Mangnus, M. J. J.; Zevenhuizen, S. J. M.; Swart, I. Mapping the Conductance of Electronically Decoupled Graphene Nanoribbons. *ACS Nano* **2018**, *12*, 7048−7056.

(9) Li, Y.; Zhang, W.; Morgenstern, M.; Mazzarello, R. Electronic and Magnetic Properties of Zigzag Graphene Nanoribbons on the (111) Surface of Cu, Ag, and Au. *Phys. Rev. Lett.* **2013**, *110*, 216804.

(10) Ijäs, M.; Ervasti, M.; Uppstu, A.; Liljeroth, P.; van der Lit, J.; Swart, I.; Harju, A. Electronic states in finite graphene nanoribbons: Effect of charging and defects. *Phys. Rev. B: Condens. Matter Mater. Phys.* **2013**, *88*, 075429.

(11) van der Lit, J.; Boneschanscher, M. P.; Vanmaekelbergh, D.; Ijäs, M.; Uppstu, A.; Ervasti, M.; Harju, A.; Liljeroth, P.; Swart, I. Suppression of electron-vibron coupling in graphene nanoribbons contacted via a single atom. *Nat. Commun.* **2013**, *4*, 2023.

(12) Baringhaus, J.; Edler, F.; Neumann, C.; Stampfer, C.; Forti, S.; Starke, U.; Tegenkamp, C. Local transport measurements on epitaxial graphene. *Appl. Phys. Lett.* **2013**, *103*, 111604.

(13) Kawai, S.; Saito, S.; Osumi, S.; Yamaguchi, S.; Foster, A. S.; Spijker, P.; Meyer, E. Atomically controlled substitutional boron-doping of graphene nanoribbons. *Nat. Commun.* **2015**, *6*, 8098.

(14) Carbonell-Sanromà, E.; Hieulle, J.; Vilas-Varela, M.; Brandimarte, P.; Iraola, M.; Barragán, A.; Li, J.; Abadia, M.; Corso, M.; Sánchez-Portal, D.; Peña, D.; Pascual, J. I. Doping of Graphene Nanoribbons via Functional Group Edge Modification. *ACS Nano* **2017**, *11*, 7355−7361.

(15) Chen, J.-H.; Jang, C.; Adam, S.; Fuhrer, M. S.; Williams, E. D.; Ishigami, M. Charged-impurity scattering in graphene. *Nat. Phys.* **2008**, *4*, 377−381.

(16) Elias, J.; Henriksen, E. Unexpected Hole Doping of Graphene by Osmium Adatoms. *Ann. Phys. (Berlin, Ger.)* **2020**, *532*, 1900294.

(17) Jia, X.; Hofmann, M.; Meunier, V.; Sumpter, B.; Campos-Delgado, J.; Romo-Herrera, J.; Son, H.; Hsieh, Y.-P.; Reina, A.; Kong, J.; Terrones, M.; Dresselhaus, M. Controlled Formation of Sharp Zigzag and Armchair Edges in Graphitic Nanoribbons. *Science* **2009**, *323*, 1701−1705.

(18) Dundas, D.; McEniry, E. J.; Todorov, T. N. Current-driven atomic waterwheels. *Nat. Nanotechnol.* **2009**, *4*, 99−102.

(19) Lü, J.-T.; Brandbyge, M.; Hedegård, P. Blowing the Fuse: Berry's Phase and Runaway Vibrations in Molecular Conductors. *Nano Lett.* **2010**, *10*, 1657−1663.

(20) Dienel, T.; Kawai, S.; Söde, H.; Feng, X.; Müllen, K.; Ruffieux, P.; Fasel, R.; Gröning, O. Resolving Atomic Connectivity in Graphene Nanostructure Junctions. *Nano Lett.* **2015**, *15*, 5185−5190.
(21) Repp, J.; Meyer, G.; Olsson, F. E.; Persson, M. Controlling the Charge State of Individual Gold Adatoms. *Science* **2004**, *305*, 493−495.
(22) Virgus, Y.; Purwanto, W.; Krakauer, H.; Zhang, S. Stability, Energetics, and Magnetic States of Cobalt Adatoms on Graphene. *Phys. Rev. Lett.* **2014**, *113*, 175502.
(23) Sevinçli, H.; Topsakal, M.; Durgun, E.; Ciraci, S. Electronic and magnetic properties of 3*d* transition-metal atom adsorbed graphene and graphene nanoribbons. *Phys. Rev. B: Condens. Matter Mater. Phys.* **2008**, *77*, 195434.
(24) Untiedt, C.; Caturla, M.; Calvo, R.; Palacios, J.; Segers, R.; van Ruitenbeek, J. Formation of a metallic contact: jump to contact revisited. *Phys. Rev. Lett.* **2007**, *98*, 206801.
(25) Kröger, J.; Jensen, H.; Berndt. Conductance of tip-surface and tip-atom junctions on Au(111) explored by a scanning tunnelling microscope. *New J. Phys.* **2007**, *9*, 153.
(26) Braun, K.-F.; Soe, W.-H.; Flipse, C. F. J.; Rieder, K.-H. Electromigration of single metal atoms observed by scanning tunneling microscopy. *Appl. Phys. Lett.* **2007**, *90*, 023118.
(27) Fernandez-Torres, L.; Sykes, E.; Nanayakkara, S.; Weiss, P. Dynamics and spectroscopy of hydrogen atoms on Pd{111}. *J. Phys. Chem. B* **2006**, *110*, 7380−7384.
(28) Repp, J.; Steurer, W.; Scivetti, I.; Persson, M.; Gross, L.; Meyer, G. Charge-State-Dependent Diffusion of Individual Gold Adatoms on Ionic Thin NaCl Films. *Phys. Rev. Lett.* **2016**, *117*, 146102.
(29) Bulou, H. Atomic diffusion on nanostructured surfaces. *Superlattices Microstruct.* **2008**, *44*, 533−541.
(30) Schulze, G.; Franke, K. J.; Pascual, J. I. Resonant heating and substrate-mediated cooling of a single C_{60} molecule in a tunnel junction. *New J. Phys.* **2008**, *10*, 065005.
(31) Schulze, G.; Franke, K. J.; Gagliardi, A.; Romano, G.; Lin, C. S.; Rosa, A. L.; Niehaus, T. A.; Frauenheim, T.; Di Carlo, A.; Pecchia, A.; Pascual, J. I. Resonant Electron Heating and Molecular Phonon Cooling in Single C_{60} Junctions. *Phys. Rev. Lett.* **2008**, *100*, 136801.
(32) Néel, N.; Limot, L.; Kröger, J.; Berndt, R. Rotation of C_{60} in a single-molecule contact. *Phys. Rev. B: Condens. Matter Mater. Phys.* **2008**, *77*, 125431.
(33) Ye, L.; Zheng, X.; Yan, Y.; Di Ventra, M. Thermodynamic meaning of local temperature of nonequilibrium open quantum systems. *Phys. Rev. B: Condens. Matter Mater. Phys.* **2016**, *94*, 245105.
(34) Erpenbeck, A.; Schinabeck, C.; Peskin, U.; Thoss, M. Current-induced bond rupture in single-molecule junctions. *Phys. Rev. B: Condens. Matter Mater. Phys.* **2018**, *97*, 235452.
(35) Preston, R. J.; Kershaw, V. F.; Kosov, D. S. Current-induced atomic motion, structural instabilities, and negative temperatures on molecule-electrode interfaces in electronic junctions. *Phys. Rev. B: Condens. Matter Mater. Phys.* **2020**, *101*, 155415.
(36) Manadé, M.; Viñes, F.; Illas, F. Transition metal adatoms on graphene: A systematic density functional study. *Carbon* **2015**, *95*, 525−534.
(37) Meair, J.; Bergfield, J. P.; Stafford, C. A.; Jacquod, P. Local temperature of out-of-equilibrium quantum electron systems. *Phys. Rev. B: Condens. Matter Mater. Phys.* **2014**, *90*, 035407.
(38) Xu, X.; Pereira, L. F. C.; Wang, Y.; Wu, J.; Zhang, K.; Zhao, X.; Bae, S.; Tinh Bui, C.; Xie, R.; Thong, J. T. L.; Hong, B. H.; Loh, K. P.; Donadio, D.; Li, B.; Özyilmaz, B. Length-dependent thermal conductivity in suspended single-layer graphene. *Nat. Commun.* **2014**, *5*, 3689.
(39) Guo, Z.; Zhang, D.; Gong, X.-G. Thermal conductivity of graphene nanoribbons. *Appl. Phys. Lett.* **2009**, *95*, 163103.
(40) Schmidt, A.; Collins, K.; Minnich, A.; Chen, G. Thermal conductance and phonon transmissivity of metal−graphite interfaces. *J. Appl. Phys.* **2010**, *107*, 104907.
(41) Néel, N.; Kröger, J.; Berndt, R. Local heating at a ferromagnet-metal interface. *Appl. Phys. Lett.* **2009**, *95*, 203103.
(42) Reif, F. *Fundamentals of Statistical and Thermal Physics*; McGraw-Hill Kogakusha, Ltd: Tokyo, 1965.
(43) Regan, B. C.; Aloni, S.; Ritchie, R. O.; Dahmen, U.; Zettl, A. Carbon nanotubes as nanoscale mass conveyors. *Nature* **2004**, *428*, 924−927.
(44) Sorbello, R. S.; Ehrenreich, H.; Spaepen, F. Theory of Electromigration. *Solid State Phys.* **1998**, *51*, 159−231.
(45) Huang, Z.; Xu, B.; Chen, Y.; Di Ventra, M.; Tao, N. Measurement of Current-Induced Local Heating in a Single Molecule Junction. *Nano Lett.* **2006**, *6*, 1240−1244.
(46) Solenov, D.; Velizhanin, K. A. Adsorbate Transport on Graphene by Electromigration. *Phys. Rev. Lett.* **2012**, *109*, 095504.
(47) Kimouche, A.; Ervasti, M. M.; Drost, R.; Halonen, S.; Harju, A.; Joensuu, P. M.; Sainio, J.; Liljeroth, P. Ultra-narrow metallic armchair graphene nanoribbons. *Nat. Commun.* **2015**, *6*, 10177.
(48) Lawrence, J.; Brandimarte, P.; Berdonces-Layunta, A.; Mohammed, M. S. G.; Grewal, A.; Leon, C. C.; Sánchez-Portal, D.; de Oteyza, D. G. Probing the Magnetism of Topological End States in 5-Armchair Graphene Nanoribbons. *ACS Nano* **2020**, *14*, 4499−4508.
(49) Talirz, L.; et al. On-Surface Synthesis and Characterization of 9-Atom Wide Armchair Graphene Nanoribbons. *ACS Nano* **2017**, *11*, 1380−1388.

https://doi.org/10.1021/acs.nanolett.1c03073
Nano Lett. 2021, 21, 8794−8799